U.S. DEPARTMENT OF THE INTERIOR
U.S. GEOLOGICAL SURVEY

Prepared for the
NATIONAL AERONAUTICS AND SPACE ADMINISTRATION

SCIENTIFIC INVESTIGATIONS MAP 2897
ATLAS OF VENUS; MEAD QUADRANGLE (V–21)
Pamphlet accompanies map

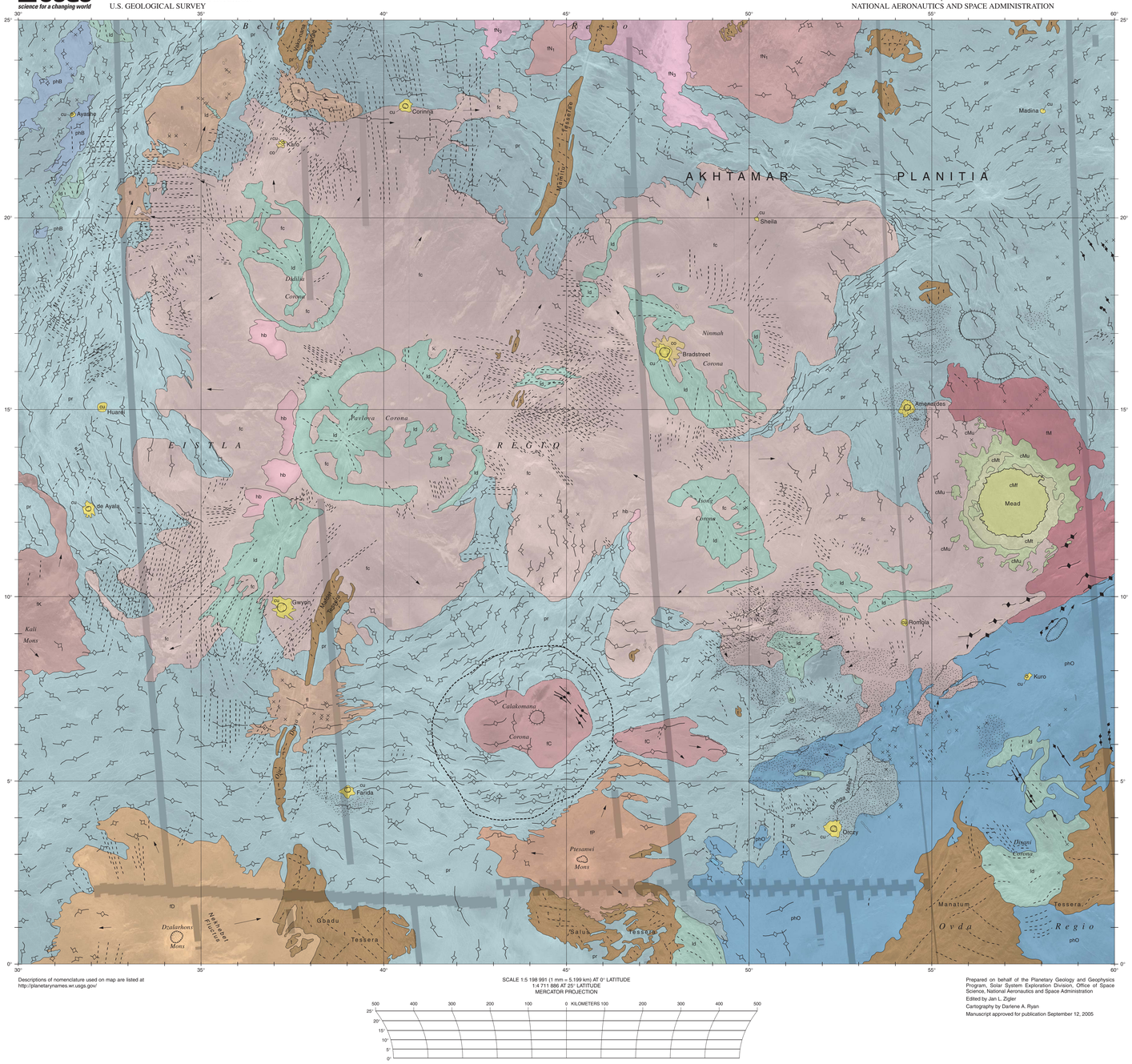

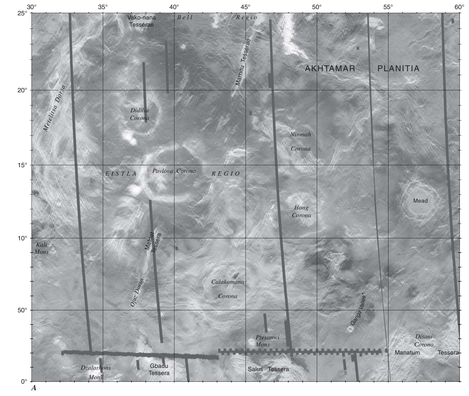

Figure 1. (***A***) Mercator projection radar image of the Mead quadrangle (V–21), Venus, showing major features. (***B***) Topographic map of Mead quadrangle with colors corresponding to planetary radius shown in perspective view. Minimum planetary radius within the quadrangle, 6,048.04 km; maximum radius, 6,054.95 km. View toward northeast.

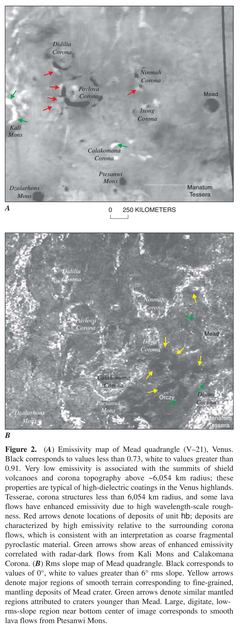

Figure 2. (***A***) Emissivity map of Mead quadrangle (V–21), Venus. Black corresponds to values less than 0.73, white to values greater than 0.91. Very low emissivity is associated with the summits of shield volcanoes and corona topography above ~6,054 km radius; these properties are typical of high-dielectric coatings in the Venus highlands. Tesserae, corona structures less than 6,054 km radius, and some lava flows have enhanced emissivity due to high wavelength-scale roughness. Red arrows denote locations of deposits of unit **hb**; deposits are characterized by high emissivity relative to the surrounding corona flows, which is consistent with an interpretation as coarse fragmental pyroclastic material. Green arrows show areas of enhanced emissivity correlated with radar-dark flows from Kali Mons and Calakomana Corona. (***B***) Rms slope map of Mead quadrangle. Black corresponds to values of 0°, white to values greater than 6° rms slope. Yellow arrows denote major regions of smooth terrain corresponding to fine-grained, mantling deposits of Mead crater. Green arrows denote similar mantled regions attributed to craters younger than Mead. Large, digitate, low-rms-slope region near bottom center of image corresponds to smooth lava flows from Pteanawi Mons.

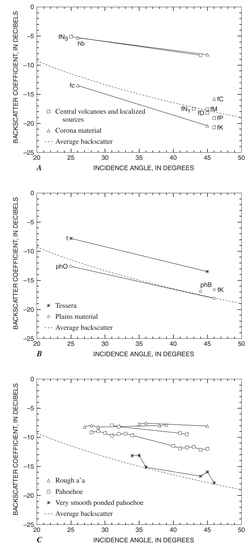

Figure 3. Radar correlation charts of selected material in Mead quadrangle (V–21), Venus, and terrestrial lavas. Average backscatter behavior of Venus surface from Muhleman law (Campbell, 1995). (***A***) Flow units of central volcanoes and localized sources, corona material; (***B***) tessera and plains material; (***C***) lava flows on Kilauea volcano, Hawaii—rough a'a, pahoehoe, and very smooth ponded pahoehoe.

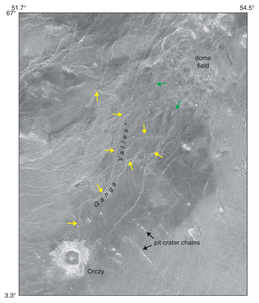

Figure 4. Magellan left-looking radar image of plains material northeast of Orczy crater in Mead quadrangle (V–21), Venus. Yellow arrows show trace of sinuous channel system (Ganga Valles*). Green arrows show trace of wider, more subdued channel structure. Dome field and pit craters may have also contributed to the broad homogeneous plains deposits in this region. North at top; image width 295 km.

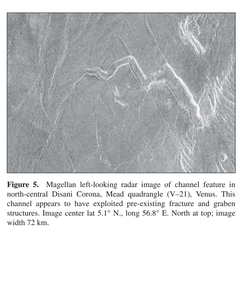

Figure 5. Magellan left-looking radar image of channel feature in north-central Disani Corona, Mead quadrangle (V–21), Venus. This channel appears to have exploited pre-existing fracture and graben structures. Image center lat 5.1° N., long 56.8° E. North at top; image width 72 km.

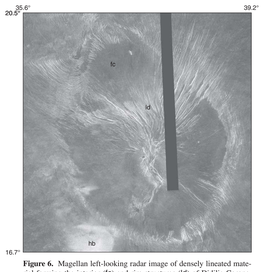

Figure 6. Magellan left-looking radar image of densely lineated material forming the interior (**fc**) and rim structures (**Id**) of Didilia Corona, Mead quadrangle (V–21), Venus. We interpret radar-bright material at lower left to be coarse pyroclastic debris (unit **hb**). North at top; image width 360 km.

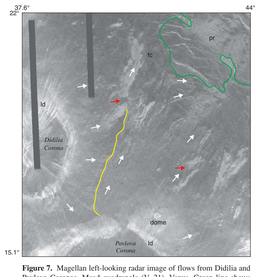

Figure 7. Magellan left-looking radar image of flows from Didilia and Pavlova Coronae, Mead quadrangle (V–21), Venus. Green line shows boundary between corona flow (unit **fc**) and regional plains (unit **pr**) materials. Yellow line shows approximate boundary of flow complexes related to the two coronae; flows from Didilia Corona end at, or are diverted by, the higher-standing Pavlova Corona flows. White arrows show flow directions. Red arrows denote proximal terminations of rough, radar-bright lava flows that are buried by younger, radar-dark materials. North at top; image width 675 km.

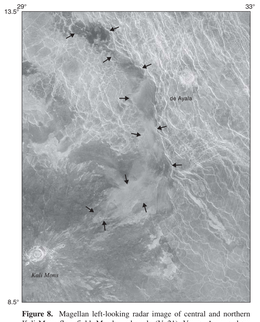

Figure 8. Magellan left-looking radar image of central and northern Kali Mons flow field, Mead quadrangle (V–21), Venus. Arrows show margins of lava flows associated with enhanced microwave emissivity (fig. 2). North at top; image width 420 km.

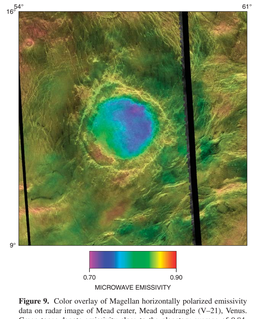

Figure 9. Color overlay of Magellan horizontally polarized emissivity data on radar image of Mead crater, Mead quadrangle (V–21), Venus. Green tones denote emissivity close to the planetary average of 0.84. Lowest value of emissivity, in northeastern portion of crater floor, about 0.72. North at top; image width 740 km.

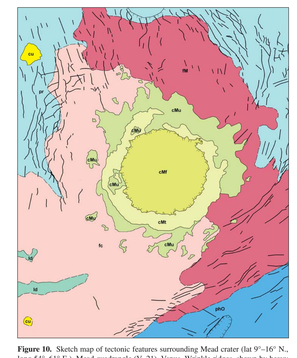

Figure 10. Sketch map of tectonic features surrounding Mead crater (lat 9°–16° N., long 54°–61° E.), Mead quadrangle (V–21), Venus. Wrinkle ridges, shown by heavy solid lines, are predominantly located on elevated terrain; ridges in the regional plains material (unit **pr**) are overlain by younger materials (units **fc** and **fM**) that embay the crater ejecta blanket. North at top; image width 740 km.

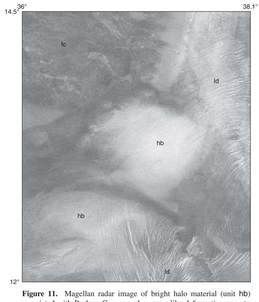

Figure 11. Magellan radar image of bright halo material (unit **hb**) associated with Pavlova Corona and a coronalike deformation zone to the southwest, Mead quadrangle (V–21), Venus. Unit designations correspond to densely lineated material (unit **Id**) and corona flow material (unit **fc**). Note radar-dark wind streaks along margins of bright regions, suggesting burial by relatively thin layers of fine material tens of centimeters thick. North at top; image width 220 km.

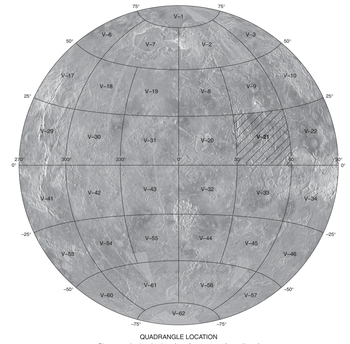

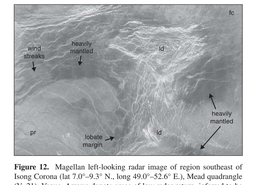

Figure 12. Magellan left-looking radar image of region southeast of Isong Corona (lat 7.0°–9.3° N., long 49.0°–52.6° E.), Mead quadrangle (V–21), Venus. Arrows denote areas of low radar return, inferred to be heavily mantled, and margins of mantling material that are lobate or conform to local topography. Unit designations correspond to densely lineated material (unit **ld**), corona flow material (unit **fc**), and regional plains material (unit **pr**). North at top; image width 380 km.

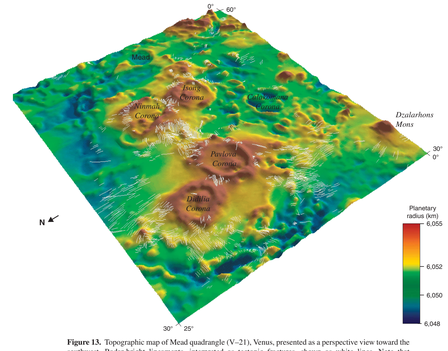

Figure 13. Topographic map of Mead quadrangle (V–21), Venus, presented as a perspective view toward the southwest. Radar-bright lineaments, interpreted as tectonic fractures, shown as white lines. Note that fractures associated with Pavlova Corona are largely confined to high-standing rim materials, while fractures associated with Didilia Corona cut both rim and flank materials.

CORRELATION OF MAP UNITS AND MAJOR EVENTS

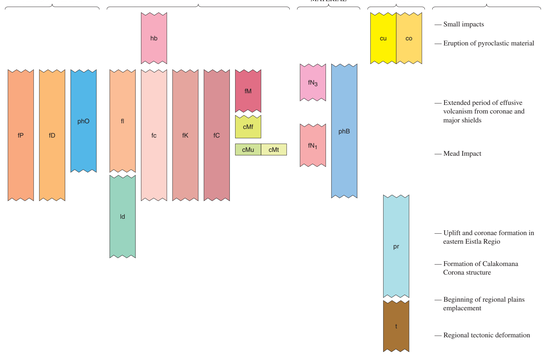

DESCRIPTION OF MAP UNITS

WESTERN OVDA REGIO MATERIAL

fP **Flow material of Ptesanwi Mons**—Low to moderate radar return; low rms slope. Lobate deposits radial to Ptesanwi Mons. Superposes regional plains material (unit **pr**) and embays north edge of Salus Tessera. At elevations above ~6,054 km radius, characterized by very high radar backscatter and low emissivity. *Interpretation*: Lava flows of relatively low surface roughness from Ptesanwi Mons. Areas of high radar backscatter and low emissivity associated with formation of surface coating or inclusions of high-dielectric phases

fD **Flow material of Dzalarhons Mons**—Low- to moderate-radar-return, moderate-rms-slope, lobate deposits radial to Dzalarhons Mons. Superposes regional plains material (unit **pr**) and embays west edge of Gbadu Tessera. At elevations above ~6,054 km radius, characterized by very high radar backscatter and low emissivity. *Interpretation*: Lava flows of moderate to high surface roughness from Dzalarhons Mons. Areas of high radar backscatter and low emissivity associated with formation of surface coating or inclusions of high-dielectric phases

phO **Homogeneous plains material of Ovda Regio**—Homogeneous radar image texture. Superposes regional plains material (unit **pr**) and embays densely lineated material (unit **ld**) in southeastern portion of quadrangle. Low- to moderate-radar-backscatter coefficient; low rms slope. Associated with numerous pit craters and small shield-like edifices. *Interpretation*: Plains formed by volcanic flooding, with relatively little post-emplacement deformation. Possible sources include Verdandi (in quadrangle V–22) and Disani Coronae and small shield volcanoes and pit craters northeast of Orczy crater

EASTERN EISTLA REGIO MATERIAL

hb **Bright halo material**—Localized deposits of very high radar return and high microwave emissivity have homogeneous appearance, with radar-dark streaks at margins and feathery edges. Superposes regional plains material (unit **pr**) and flow materials of coronae (unit **fc**); primarily occurs on exterior corona flank slopes, with at least one point of contact with densely lineated material (unit **ld**). *Interpretation*: Rough pyroclastic material erupted in most recent period of corona volcanism, likely by a ground-hugging surge mechanism rather than by airfall. Radar-dark streaks likely wind-deposited, fine material that blankets rough surface

fl **Localized flow material**—Lobate deposits radiating from a central depression, low-relief dome, or chain of small domes in the plains. Typically less than 200 km in radial extent; variable radar brightness. Superposes regional plains material (unit **pr**). In northwestern portion of quadrangle, superposed by lobate materials of unit **fc**. *Interpretation*: Lava flows associated with small shield volcanoes and calderas in the plains

fc **Flow material of coronae**—Low- to moderate-radar-return deposits radial to coronae and corona-like deformation patterns in eastern Eistla Regio. Morphology varies from sheetlike to narrow lobes. Embays tectonically deformed rim and central corona structures; superposes regional plains material (unit **pr**); topographically, is confined to south by deformation associated with Calakomana Corona. For Didilia and Pavlova Coronae, narrow, lobate, radar-bright deposits are stratigraphically lower; later materials form low-radar-return, sheetlike aprons that embay and flood earlier lobate terrain. *Interpretation*: Lava flows erupted in association with corona formation. Relative age of flows from individual coronae, in general, indeterminate. For Didilia and Pavlova Coronae, earlier eruptions appear to have higher volume or are more viscous, while later eruptions are characterized by lower eruption rate or lower viscosity

fK **Flow material of Kali Mons**—Low- to moderate-radar-return, lobate deposits radial to Kali Mons. Superposes regional plains material (unit **pr**). To the northeast, characterized by moderate to low radar backscatter and enhanced emissivity. *Interpretation*: Lava flows from Kali Mons. Areas of enhanced emissivity may indicate a low-density, surface-mantling deposit or highly vesicular lava flow texture

fC **Flow material of Calakomana Corona**—Low- to moderate-radar-return, lobate, and mottled deposits interior to Calakomana Corona, with low domical edifice in center of deposit; moderate-radar-return, lobate deposits east of Calakomana that superpose local structure and regional plains material (unit **pr**). *Interpretation*: Lava flows related to Calakomana Corona

fM **Flow material near Mead crater**—Moderate- to low-radar-backscatter, low-rms-slope deposits that embay Mead crater ejecta (units **cMu**, **cMf**) along north, south, and east sides of crater. Image texture often featureless. Superposes regional plains material (unit **pr**), wrinkle ridges, pit craters, and other features in low terrain surrounding Mead crater. Contact with unit **fc** uncertain and likely controlled by topography. *Interpretation*: Lava flows generated by volcanic sources north and east of Mead crater

cMf **Mead crater floor material**—Moderate-radar-return, patchy image texture; emissivity lower than planetary average in eastern portion of crater. Central region characterized by short, radar-bright lineaments; margins characterized by localized lobate or patchy variations in radar brightness. *Interpretation*: Impact melt sheet formed during impact event or post-excavation lava flows. Crater floor lineaments may reflect fracturing of deposit during cooling. Low emissivity suggests modest increase in bulk dielectric constant relative to planetary average

cMu **Mead crater distal ejecta material**—Radar-bright hummocky or patchy terrain. Features typically radial to Mead crater. Superposes unit **pr**; embayed by units **fc** and **fM**. *Interpretation*: Rugged ejecta from Mead crater impact event, embayed by later flows from corona to the west and other sources east and north of the crater

cMt **Mead crater terrace material**—Moderate to low radar return; mottled image texture. Occurs on gently sloped terrain concentric to Mead crater floor. *Interpretation*: Topographic terrace formed as part of collapse of Mead crater cavity during impact event. Surface materials likely represent overturned target terrain, because low-emissivity signature associated with crater floor material (unit **cMf**) is not evident

ld **Densely lineated material**—Bright radar return, with typically single principal lineament orientation. Forms parts of corona rim deposits. Occurs as isolated outcrops embayed by regional plains (unit **pr**) and corona flow materials (unit **fc**). *Interpretation*: Material of uncertain origin (though likely regional plains, unit **pr**) that has been pervasively deformed by compression

SOUTHERN BELL REGIO MATERIAL

fN$_3$ **Upper flow material of Nyx Mons**—Complex of radar-bright, lobate-margined deposits that is typically radial to Nyx Mons. Superposes radar-dark material of units **fN$_1$** and **fN$_2$** (in quadrangle V–9) and regional plains material (unit **pr**) to the south. *Interpretation*: Lava flows from a variety of source vents associated with Nyx Mons that postdate unit **pr** and the materials of units **fN$_1$** and **fN$_2$**. Enhanced radar backscatter likely due to rough surface texture at the 12.6-cm scale of the illuminating wavelength

fN$_1$ **Lower flow material of Nyx Mons**—Low- to moderate-radar-return, lobate, and sheet-like deposits radial to Nyx Mons. Superposes regional plains material (unit **pr**) and tessera material to the south. *Interpretation*: Lava flows from Nyx Mons that postdate unit **pr**. Backscatter coefficients are consistent with terrestrial, smooth pahoehoe flows

phB **Homogeneous plains material of Bell Regio**—Homogeneous radar image texture. Superposes regional plains material (unit **pr**) in northwest corner of quadrangle. Moderate radar backscatter coefficient; low rms slope. *Interpretation*: Moderately rough plains formed by volcanic flooding, with relatively little post-emplacement deformation

WIDESPREAD MATERIAL

cu **Crater material, undifferentiated**—Radar-bright material surrounding a central depression, rim materials, and floor materials of radar-bright and radar-dark varieties; exterior deposits typically lobate, with patchy radar image texture and bright streaks radial to the central cavity. Superposes surrounding units. *Interpretation*: Crater formed by impact. Hummocky texture of near-rim material reflects distribution of continuous ejecta. Radar-bright floors may be fractured impact melt, while radar-dark floors may reflect post-emplacement volcanic flooding or smooth impact melt

co **Crater outflow material**—Mottled or swirled radar image texture, with lobate margins and streaks parallel to the downhill direction; typically of moderate radar brightness. Superposes surrounding units and crater material, undifferentiated (unit **cu**). *Interpretation*: Melt generated by the impact event escapes from the crater cavity to form a lavalike flow deposit

pr **Regional plains material**—Radar backscatter properties variable due to density of ridges, but background terrain characterized by moderate to low radar backscatter, low rms slope. Embays tessera and densely lineated material. High density of wrinkle ridges or fractures. *Interpretation*: Smooth complexes of sheetlike or flood lavas that have undergone extensive tectonic deformation and formation of coronae and coronalike annular features

t **Tessera material**—Radar-bright regions elevated relative to, and embayed by, regional plains material (unit **pr**), flow material of coronae (unit **fc**), and edifices; abundant fractures, ridges, and graben with multiple principal orientations. *Interpretation*: Highly deformed terrain. Original nature of material indeterminate. Relative ages of isolated tessera outcrops indeterminate, but trend and shape of Gbadu and Mamitu Tesserae similar to outcrops southwest and west of Bell Regio suggest a shared contractional regime

Contact—Dashed where approximately located

Sinuous rille

Fracture

Wrinkle ridge

Ridge

Graben

Calakomana Corona boundary

Flow direction

Dome

Dome or circular scarp—Hachures point downslope

Caldera or pit crater

Crater rim showing crest

Chain craters

Surficial materials—Fine-grained material, likely produced by impact events, that mantles the underlying surface and reduces backscatter return. Radar-dark deposits with feathery margins occur as regional deposits, linear or arcuate streaks, and accumulations along east edges of topographic features such as wrinkle ridges

*Name provisionally accepted by International Astronomical Union

[1]Center for Earth and Planetary Studies, Smithsonian Institution, Washington, DC
[2]Department of Mathematics, University of California, San Diego, CA

Geologic Map of the Mead Quadrangle (V–21), Venus

By
Bruce A. Campbell[1] and David A. Clark[2]

2006

For sale by U.S. Geological Survey, Information Services, Box 25286, Federal Center, Denver, CO 80225, 1-888-ASK-USGS
Available on World Wide Web at http://pubs.usgs.gov/sim/2006/2897

ISBN 1-411-30995-2